Eddington ratio and accretion efficiency in AGN evolution

S.I. Raimundo* and A.C. Fabian
Institute of Astronomy, Madingley Road, Cambridge CB3 0HA

25 March 2009

ABSTRACT
The cosmological evolution of Active Galactic Nuclei (AGN) is important for understanding the mechanism of accretion onto supermassive black holes, and the related evolution of the host galaxy. In this work, we include objects with very low Eddington ratio ($10^{-3} - 10^{-2}$) in an evolution scenario, and compare the results with the observed local distribution of black holes. We test several possibilities for the AGN population, considering obscuration and dependence with luminosity, and investigate the role of the Eddington ratio λ and radiative accretion efficiency ϵ on the shape of the evolved mass function. We find that three distinct populations of AGN can evolve with a wider parameter range than is usually considered, and still be consistent with the local mass function. In general, the black holes in our solutions are spinning rapidly. Taking fixed values for ϵ and λ neither provides a full knowledge of the evolution mechanism nor is consistent with the existence of low Eddington ratio objects.

Key words: galaxies: nuclei - galaxies: active - quasars: general - black hole physics

1 INTRODUCTION

Understanding how Active Galactic Nuclei (AGN) work has been a major goal since the discovery of quasars (Schmidt 1963). It is now believed that mass accretion onto a supermassive black hole (SMBH) is the mechanism that powers AGN (Salpeter 1964; Lynden-Bell 1969; Rees 1984), and this hypothesis is supported by recent evidence for massive black holes in the centre of most nearby galaxies (Kormendy & Richstone 1995; Richstone et al. 1998). The mass of the black hole (BH) is related to the properties of the host galaxy (Magorrian et al. 1998; Marconi & Hunt 2003), implying a close relation between the evolution of galaxies and the BH in their centres.

Soltan (1982), developed a method to obtain the total mass density of SMBH, $\rho_{\rm BH}$, from the emitted light and number counts of AGN, providing a way to trace the accretion history of these BHs, from the AGN luminosity function as a function of redshift. Following this approach, there have been attempts to compute the evolution of the BH mass function from a starting redshift, and compare it with the BH distribution in nearby galaxies, known as the local distribution (Small & Blandford 1992; Salucci et al. 1999; Marconi et al. 2004; Merloni 2004; Shankar, Weinberg, & Miralda-Escudé 2007). Progress has been made by the use of semi-analytical models and increasingly better observational results, although it is still hard to constrain the important factors affecting this calculation: the luminosity function at each redshift, the bolometric correction, the obscuration and the free parameters related with the accretion process.

There is evidence from the X-ray background that obscuration plays an important role in AGN evolution. The background is due to the integrated emission from AGN with high intrinsic absorption (e.g. Brandt & Hasinger 2005), and by modelling it, Fabian & Iwasawa (1999) found that most of the accretion onto AGN is obscured. One of the main goals of AGN studies is to get unbiased samples of objects, and for this, X-ray surveys reveal more AGN than found in other wavelength bands. The observations in the hard X-ray band (2-10 keV) are the least biased against obscuration, and therefore more suitable to observe and study AGN. Ueda et al. 2003 (hereafter U03) show that the hard X-ray luminosity function is best-fitted by a luminosity dependent density evolution (LDDE), and that the number density of low luminosity AGN peaks at lower redshift than the high luminosity ones. To be able to convert the X-ray to total energy output, and obtain a knowledge of the multi-wavelength properties, a bolometric correction is needed, this is a function of source luminosity (e.g., Marconi et al. 2004), or more likely, the Eddington ratio (Vasudevan & Fabian 2007).

The accretion mechanism is another important factor. There are two important free parameters to describe it; one, the radiative accretion efficiency ϵ, representing the fraction of accreted mass radiated, establishes the relation between the bolometric luminosity and the growth rate of the BH, the other, the Eddington ratio λ, relates the AGN bolometric luminosity with the Eddington luminosity: $L = \lambda L_{\rm E}$, with $L_{\rm E} = 4\pi c G M m_{\rm H}/\sigma_{\rm T}$. In previous work, the Eddington ratio has been taken to be either a constant, changing as a function of redshift, or a function of mass (see Shankar et al. 2007 and references therein).

Another factor is the hydrogen column density ($N_{\rm H}$) distribution, often called the $N_{\rm H}$ function. Several studies tried to parametrise it, U03 showed that the absorption is luminosity dependent, with $N_{\rm H}$ a decreasing function of the intrinsic luminosity, and found no significant dependence on redshift, although this question

* E-mail: sijr@ast.cam.ac.uk

is still in debate (see for example Tozzi et al. 2006; Treister & Urry 2006).

To constrain the parameters involved in the growth of AGN, Marconi et al. (2004) compare the mass function from AGN relics with the local mass function, using a single AGN population. They find an acceptable match for $0.1 \leq \lambda \leq 1.7$, and $0.04 \leq \epsilon \leq 0.16$, with the values $\epsilon = 0.08$ and $\lambda = 0.5$ giving the minimum deviation between the two mass functions. However, recent results showed that the Eddington ratio can be significantly lower, with many objects having $\lambda \sim 10^{-2} - 10^{-3}$, (Babić et al. 2007; Fabian, Vasudevan, & Gandhi 2008), at least one order of magnitude less than the Marconi et al. (2004) lowest acceptable value. This indicates that there is a wide spread in the range of λ, and that we have to consider low values for this parameter when computing the AGN mass function.

In this paper, we analyse how the free parameters λ and ϵ influence the shape of the evolved AGN mass function, starting by considering one population of AGN, which is then split in two, according to obscuration. This leads to an implausible excess of high mass objects so we add a luminosity dependence for AGN with low λ, and consider the evolution of *three* different populations. The real situation is undoubtedly more complex than our simple models, but we expect to have captured the essence of AGN evolution in the (ϵ, λ) plane.

We adopt standard cosmological parameters of $H_0 = 70$ km s^{-1} Mpc^{-1}, $\Omega_m = 0.3$ and $\Omega_\Lambda = 0.7$.

2   THE BLACK HOLE MASS FUNCTION

To obtain a black hole mass function for $z = 0$, and compare it with the local observed mass function, we follow the procedure of Marconi et al. (2004) (hereafter M04) and Shankar et al. (2007). Starting with an AGN luminosity function (LF) at certain redshift z_i, and considering that all BHs were active, we follow their evolution with cosmic time, assuming that their growth and energy output are due to mass accretion only.

Using Soltan's argument (1982), we can establish a relation between the total energy output, given by the integrated luminosity function, and the density of BH:

$$\rho_{BH} = \frac{1-\epsilon}{\epsilon c^2 \ln 10} \int_0^{z_i} \frac{dt}{dz} dz \int_{L_1}^{L_2} \frac{\partial \phi(L,z)}{\partial \log L} dL.$$

Here, L is the bolometric luminosity, ϵ the radiative accretion efficiency and:

$$\frac{dt}{dz} = - \left[(1+z) H_0 \sqrt{(1+z)^3 \Omega_m + \Omega_\lambda} \right]^{-1},$$

for the cosmological model used in this work. We are interested in the AGN distribution of masses, i.e., what is the number of objects with a certain mass M, per unit of comoving volume, and how it varies with redshift. For this, we use the continuity equation for the non-merging case, (see Cavaliere, Morrison, & Wood 1971; Small & Blandford 1992). Considering that the BH growth is only due to mass accretion, we assume that the total number of BHs is constant with time, and obtain:

$$\frac{\partial}{\partial t} \frac{\partial \phi(M,t)}{\partial M} + \frac{\partial}{\partial M} \left[\frac{\partial \phi(M,t)}{\partial M} \langle \dot{M}(M,t) \rangle \right] = 0. \qquad (1)$$

In the case of merging, the right side of the continuity equation would not be zero, but equal to a source function, implying that the total number of BHs is not conserved. In Eq. 1, $\phi(M,t)$ is the number of BH with mass M per unit comoving volume for a certain

cosmic time t and $\langle \dot{M}(M,t) \rangle$ is the mean accretion rate for BH of mass M (active and inactive):

$$\langle \dot{M}(M,t) \rangle = \delta(M,t) \dot{M}(M,t). \qquad (2)$$

Here $\delta(M,t)$ is the fraction of active (accreting) BH as a function of M and t, called the duty cycle. $\dot{M}(M,t)$ is the accretion rate (or growth rate) of a BH with mass M at time t.

The growth rate is a result of the mass that falls to the BH but is not converted into energy (see Marconi et al. 2004). If we have a total mass falling ($\dot{M}_{tot}$), part of it is converted into energy $L = \epsilon \dot{M}_{tot} c^2$, and the rest will accrete onto the BH: $\dot{M} = (1-\epsilon) \dot{M}_{tot}$. Consequently,

$$L = \frac{\epsilon}{(1-\epsilon)} c^2 \dot{M}(M,t).$$

The energy output at a certain t is due to active BHs, so

$$\frac{d\phi(L,t)}{d \log L} d \log L = \delta(M,t) \frac{d\phi(M,t)}{dM} dM. \qquad (3)$$

Using Eq. 2 and Eq. 3 to eliminate $\delta(M,t)$, and replacing in the continuity equation (1)

$$\frac{\partial}{\partial t} \frac{\partial \phi(M,t)}{\partial M} + \frac{\partial}{\partial M} \left[\frac{d\phi(L,t)}{d \log L} \frac{d \log L}{dM} \dot{M}(M,t) \right] = 0.$$

L and M are related by $L = \frac{\lambda c^2}{t_E} M$, with $t_E = \frac{\sigma_T c}{4 \pi G m_H}$, and assuming constant Eddington ratio (λ) and ϵ, one can solve the continuity equation to obtain the mass function at a redshift z_f:

$$\frac{d\phi(M,z_f)}{dM} = \frac{(1-\epsilon)\lambda^2 c^2}{\epsilon t_E^2 \ln 10} \int_{z_f}^{z_i} \frac{\partial}{\partial L} \left[\frac{d\phi(L,z)}{d \log L} \right] \left| \frac{dt}{dz} \right| dz \qquad (4)$$

This equation tells us that the mass function at a certain redshift, can be obtained with a Soltan-type argument, by tracking the energy that was produced due to mass accretion from z_i to z_f. We assume that the initial mass function (at redshift 3), does not contribute significantly to the final mass function, since the major black hole growth occurs for $z < 3$ (M04).

To be able to compare this evolved mass function with the local one, the previous equation has to be evaluated for $z_f = 0$. We have to assume a certain luminosity function, a bolometric correction, set the initial conditions and give values to ϵ and λ. For the LF, we consider the luminosity-dependent density evolution (LDDE) of U03, which describes $\frac{\partial \phi(L_X, z)}{\partial \log L_X}$, the number of AGN with intrinsic luminosity L_X per unit of comoving volume per $\log L_X$, as function of the luminosity and the redshift:

$$\frac{d\phi(L_X, z)}{d \log L_X} = A \left[\left(\frac{L_X}{L_\star} \right)^{\gamma_1} + \left(\frac{L_X}{L_\star} \right)^{\gamma_2} \right]^{-1} e(z, L_X),$$

where $e(z, L_X)$ is the evolution term,

$$e(z, L_X) = \begin{cases} (1+z)^{p_1} & z < z_c(L_X), \\ [1+z_c(L_X)]^{p_1 - p_2}(1+z)^{p_2} & z \geq z_c(L_X), \end{cases}$$

and the redshift cut off,

$$z_c(L_X) = \begin{cases} z_c^\star & L_X \geq L_a, \\ z_c^\star \left(\frac{L_X}{L_a} \right)^\alpha & L_X < L_a. \end{cases}$$

The parameters have the values: A $= 5.04 \times 10^{-6}$ Mpc^{-3}; $L_a = 10^{44.6}$ erg s^{-1}; $L_\star = 10^{43.94}$ erg s^{-1}; $\gamma_1 = 0.86$; $\gamma_2 = 2.23$; $p_1 = 4.23$; $p_2 = -1.5$; $z_c^\star = 1.9$; $\alpha = 0.335$. This luminosity function has a discontinuity in its derivative, which leads to unphysical solutions for the mass function. To avoid that, we rewrite the luminosity function to make it continuous in its derivatives (A. Marconi, private

communication):

$$\frac{d\phi(L_X, t)}{d \log L_X} = \left[\left(\frac{d\phi(L_X \geq L_a, t)}{d \log L_X} \right)^{-\beta} + \left(\frac{d\phi(L_X < L_a, t)}{d \log L_X} \right)^{-\beta} \right]^{-\frac{1}{\beta}}$$

with $\beta = 8$.

For the bolometric luminosity L, we use the Eddington ratio dependent bolometric correction $\kappa(\lambda) = L/L_X$ (Vasudevan & Fabian 2007), with $\kappa(\lambda) = 19.3$ for $\lambda \leq 0.1$, $\kappa(\lambda) = 54.5$ for $\lambda \geq 0.3$, and an intermediate value of $\kappa(\lambda) = 36.9$ for the other Eddington ratios. To account for Compton-thick AGN, we multiply our mass function by a constant factor of 1.6, following the result by Risaliti et al. (1999). In this work we consider $z_i = 3$, and that all BHs were active at that time ($\delta(M, z_i) = 1$). Using

$$\frac{d\phi(L, z)}{d \log L} d \log L = \frac{d\phi(L_X, z)}{d \log L_X} d \log L_X,$$

and since $\kappa(\lambda)$ is constant for an assumed value of λ, we finally obtain

$$\frac{d\phi(M, 0)}{dM} M = \frac{(1 - \epsilon)\lambda L}{\epsilon t_E \ln 10} \int_0^3 \frac{\partial}{\partial L} \left[\frac{d\phi(L_X, z)}{d \log L_X} \right] \times \left| \frac{dt}{dz} \right| dz. \quad (5)$$

For a simple model of one population of AGN, we apply the method described before, noting that each set of parameters λ and ϵ give a different mass function for the same luminosity. To add the effect of obscuration, and understand the role of the absorbed AGN in the shape of the mass function, we consider the AGN population to be separated in two groups with different absorption column densities N_H: unabsorbed ($10^{20} \text{cm}^{-2} \leq N_H < 10^{22} \text{cm}^{-2}$), and absorbed ($10^{22} \text{cm}^{-2} \leq N_H < 10^{24} \text{cm}^{-2}$). We define

$$\mathcal{N}_H(L_X) = \int_{N_1}^{N_2} f(L_X; N_H) d \log N_H, \quad (6)$$

where $f(L_X; N_H)$ is the probability distribution function from U03, normalised to unity in the Compton-thin region $20.0 \leq \log N_H \leq 24.0$. We find $\mathcal{N}_H^{abs}(L_X)$ integrating Eq. 6 between the values of column density assumed for absorbed AGN, and $\mathcal{N}_H^{un}(L_X)$ integrating in a similar way for the unabsorbed ones. That is, for each value of L_X, we split our population in two groups, with constant number fractions given by the $\mathcal{N}_H(L_X)$ function. In summary we have:

$$\frac{d\phi(M, 0)}{dM}^{abs} = \mathcal{N}_H^{abs}(L_X) \times \frac{d\phi(M, 0)}{dM}, \quad (7)$$

$$\frac{d\phi(M, 0)}{dM}^{un} = \mathcal{N}_H^{un}(L_X) \times \frac{d\phi(M, 0)}{dM}. \quad (8)$$

3 CONSTRAINTS ON THE FREE PARAMETERS

To constrain the free parameters λ and ϵ, we compare our evolved AGN mass function with the local mass function. As a reference, we use the local mass function in M04 and the respective 1σ error, in the range $(10^6 - 10^{10}) M_\odot$ which was obtained using both the $M_{BH} - \sigma_*$ (velocity dispersion), and the $M_{BH} - L_{bul}$ (bulge luminosity) relations. The method to obtain the mass function is as follows: for each mass value, we compute the corresponding L_X by first using $L = \lambda L_E$ to obtain the bolometric luminosity from the mass, and then $\kappa(\lambda)$ to convert from bolometric to intrinsic luminosity. We then replace the U03 luminosity function and the bolometric correction in Eq. 5, differentiate in L and integrate
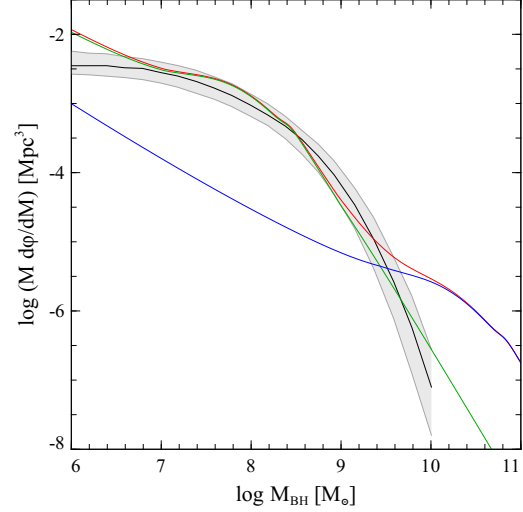

Figure 1. Comparison between the evolved number of AGN per unit volume and the local mass function (in black) by Marconi et al. (2004). The grey area is the 1σ error in the M04 local mass function. The green curve represents the unabsorbed AGN, and the blue curve the absorbed AGN. The red curve is the total population (absorbed plus unabsorbed). The values used were $\lambda_{abs} = 10^{-3}$, $\epsilon_{abs} = 0.085$, $\lambda_{un} = 0.56$, $\epsilon_{un} = 0.21$ with the Ueda et al. (2003) N_H distribution. For a low value of λ, a two population model predicts a higher number of high mass black holes than that observed.

from $z = 0$ to $z = 3$ to obtain $\frac{d\phi(M, 0)}{dM}$. For the case of two or more populations we use Eq. 6 to compute the $\mathcal{N}_H$ function for each value of L_X, and replace it in Eq. 7 for the absorbed and Eq. 8 for the unabsorbed, allowing each population to have a different Eddington ratio and accretion efficiency.

For one population, with only two free parameters, we find no value of ϵ or λ for which the evolved mass function is consistent with the local one within a 1σ error. Considering a black hole mass range of $(10^7 - 10^9) M_\odot$, we obtain agreement but only for high Eddington ratios ($\lambda > 0.1$). To search for alternative scenarios and be able to have lower λ we study the effect of obscuration, by considering the N_H function by U03.

3.1 Two populations

We start by assuming two populations, one of obscured and one of unobscured AGN. The agreement between the local and the evolved number density of AGN can be obtained by changing simultaneously the free parameters for the absorbed and unabsorbed objects. To constrain the allowed ranges for the accretion efficiency and the Eddington ratio, we search parameter space, find the evolved number density of AGN for every combination of the four parameters ($\lambda_{abs}, \epsilon_{abs}, \lambda_{un}, \epsilon_{un}$), and compare it with the local number density from M04. We search the parameter range: $10^{-3} \leq \lambda \leq 1$, $10^{-2} \leq \epsilon \leq 0.42$. The upper value of ϵ is limited by the maximum accretion onto a Kerr black hole, if we consider a case of a radiatively efficient system, the radiative accretion efficiency ϵ is equal to the mass to energy efficiency (η). In a more general case, $\epsilon \leq \eta$.

With two populations, we do not find parameters that result in a mass function within 1σ of the local mass function. We only find good agreement if we limit the mass range to $M_{BH} = (10^7 - 10^9) M_\odot$, but for low values of λ, it predicts a higher density of high mass black holes ($> 10^9 M_\odot$) than that observed, which is

not consistent. In Fig. 1 we chose a set of values to illustrate our problem, the total mass function in red is compared with the local mass function from M04. The blue and green lines represent the absorbed and unabsorbed populations respectively, with fixed parameters. For low values of λ, although it is possible to obtain good agreement in a limited mass range, the sum of the absorbed and unabsorbed populations (red line), predicts a higher number of high mass black holes than observed. This is a common problem, both for M04 luminosity dependent and Vasudevan & Fabian (2007) Eddington ratio dependent bolometric corrections. When λ is lowered ($\lambda < 10^{-2}$), the mass function shifts down and right, which means that it raises the number density of high mass black holes. Nevertheless, low λ objects are observed in the Universe, and we require that they agree with the local mass function.

3.2   Three populations

To obtain agreement in the high mass black hole range, the number of AGN with low Eddington ratio has to drop with luminosity. By hypothesis, and in agreement with the N_H function in U03, we assume that the low λ objects are included in the obscured population. We therefore divide our absorbed population in two: the absorbed objects with lower Eddington ratio ($10^{-3} < \lambda < 10^{-2}$), and objects with higher Eddington ratio ($10^{-2} < \lambda < 1$). This way, our AGN population is divided into three groups: obscured objects with lower λ and numbers dropping with increasing luminosity, obscured objects with higher λ, and unobscured objects ($10^{-2} < \lambda < 1$).

For the luminosity dependence, we define a simple decay for the fraction $f(L_X)$, the number of objects with low λ divided by the total number of absorbed objects for a certain luminosity:

$$f(L_X) = S \log(L_X) + b,$$

where S is the free parameter, and b is determined by assuming that for $L_X < 10^{41} \mathrm{erg}\, s^{-1}$ all the absorbed AGN have low λ ($f = 1$). Therefore, the mass functions for the three populations are:
- Absorbed with low λ:

$$\frac{d\phi(M,0)}{dM}^{\text{labs}} = f(L_X) \times \mathcal{N}_H^{\text{abs}}(L_X) \times \frac{d\phi(M,0)}{dM} \qquad (9)$$

- Absorbed:

$$\frac{d\phi(M,0)}{dM}^{\text{abs}} = (1 - f(L_X)) \times \mathcal{N}_H^{\text{abs}}(L_X) \times \frac{d\phi(M,0)}{dM} \qquad (10)$$

- Unabsorbed:

$$\frac{d\phi(M,0)}{dM}^{\text{un}} = \mathcal{N}_H^{\text{un}}(L_X) \times \frac{d\phi(M,0)}{dM} \qquad (11)$$

In terms of free parameters, we now have ($\lambda_{\text{abs}}, \epsilon_{\text{abs}}, \lambda_{\text{un}}, \epsilon_{\text{un}}, \lambda_{\text{labs}}, \epsilon_{\text{labs}}, S$). Following this method, we find several sets of parameters for which there is good agreement with the local mass function. In Fig. 2 we have an example of a set of parameters for which there is good agreement, the grey area is the 1σ error of the M04 local mass function (in black) and the red line is our total evolved mass function. The green line represents the unabsorbed population, and the blue lines the absorbed: light blue for the low λ and dark blue for the others. As we can see, a decay in f with luminosity allows the low λ population to agree in the high black hole mass range, and we obtain very good agreement between our evolved mass function and the local one. In terms of the effect of a parameter change, lowering ϵ, makes the mass growth of the BHs more efficient, and the curves in Fig. 2 go up. λ shifts the curves to the high
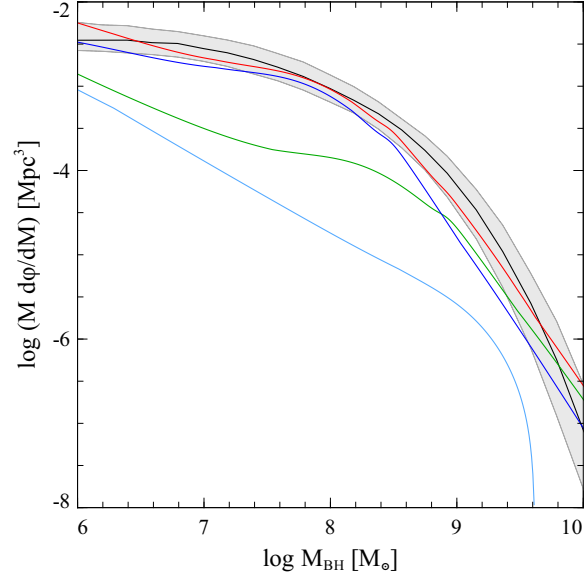

Figure 2. Comparison between the evolved number of AGN per unit volume and the local mass function (in black) by Marconi et al. (2004). The grey area is the 1σ error in the M04 local mass function. The green curve represents the unabsorbed AGN, and the blue curves the absorbed AGN: light blue for the absorbed objects with low λ and dark blue for the others. The red curve is the total population (absorbed, absorbed low λ and unabsorbed). The values used were $\lambda_{\text{labs}} = 0.007$, $\epsilon_{\text{labs}} = 0.21$, $\lambda_{\text{abs}} = 0.5$, $\epsilon_{\text{abs}} = 0.068$, $\lambda_{\text{un}} = 0.079$, $\epsilon_{\text{un}} = 0.21$ and $S = -0.3$ with the Ueda et al. (2003) N_H distribution.

mass or low mass end. An increase in λ corresponds to a shift to the left and up, a decrease makes the curves go right and down. The plot in Fig. 3 shows the result of our search in the parameter range described for the two populations and also with $10^{-3} < \lambda_{\text{labs}} < 10^{-2}$, $10^{-2} < \epsilon_{\text{labs}} < 0.42$ and $-1 < S < 0$. Each population is described by a set of three points in the plot: light blue (light grey), dark blue (black) and green (medium grey). The sum of these three populations gives the total one, which is evolved and compared with the local mass function. We plot all the values of λ and ϵ for which the evolved mass function is within a 1σ error from the local one. Note that the number of points are not the same for all populations because an unabsorbed population can have, for example, more than one absorbed or low lambda absorbed population for which the mass function agrees well with the local one.

In terms of the general features, we see that we obtain a wide range of possible parameters. Each population is described by a point in Fig. 3, which means that the total mass function (red line on the previous plots), is described by a definite set of three points, light blue (light grey), dark blue (black) and green (medium grey), and not a random combination. The absorbed and unabsorbed, blue (light grey and black) and green (black), populations, have values of λ that are in general higher that 0.1, and the absorbed with low λ, light blue (light grey), spread in the whole parameter range ($10^{-3} - 10^{-2}$). We notice a void, due to the fact that for the absorbed with high λ and unabsorbed, an Eddington ratio $\gtrsim 0.1$ causes the evolved mass function to disagree from the local mass function in the high mass range. Allowing the Eddington ratio for the low λ absorbed objects to go higher than 10^{-2} would fill in the void. Values for the slope S, are found between -0.75 and -0.25, which means that the values for the luminosity L_X where f reaches zero range from $10^{42.3} \mathrm{erg}\, s^{-1}$ to $10^{45} \mathrm{erg}\, s^{-1}$. These values corre-

spond to a steeper decay than for example the absorbed fractions from Hasinger (2008) or Treister et al. (2008), which combine absorbed objects of all λ. The values for the accretion efficiency are above 0.035, and in this scenario, lower for absorbed objects than unabsorbed objects in the same range of λ. We do not find evidence for advection dominated accretion flows (ADAF) behaviour in our low efficiency objects. As we can see from Fig 3, almost all possible parameters are above $\epsilon = 0.057$, which is the efficiency corresponding to a Schwarzschild (non-rotating) black hole, indicating that the black holes must be spinning. In fact, most of the black holes in our solutions are rapidly spinning. A population of low λ objects with low efficiency, light blue (light grey) points, or low efficiency absorbed objects, dark blue (black) points, can only represent the local mass function if combined with unabsorbed, green (medium grey), objects with high efficiencies ($\epsilon > 0.1$).

We have assumed that Compton-thick objects contribute to the mass function equally in all the mass range, and set a correction factor of 1.6 to account for them. A change in this value would not affect qualitatively the shape of the relation between ϵ and λ showed in Fig. 3. To evaluate the errors, we used two approaches: a higher multiplying correction factor and a similar method to Gilli et al. (2007). In terms of the mass functions, a higher multiplying factor shifts all the curves up, making the lower values of ϵ in Fig. 3 be inconsistent with the local mass function. In summary, a higher fraction of Compton-thick objects would imply that the local mass function can be reproduced using higher accretion efficiencies than the ones from Fig. 3. For the Gilli et al. (2007) N_H function, we obtain results that do not differ significantly from the ones with the U03 N_H function, the main difference is that the parameter values for the absorbed objects (high λ), are found in the same range as the unabsorbed, that is, higher than the ones from U03.

4 SUMMARY AND CONCLUSIONS

We have tried to reconcile the existence of low Eddington ratio AGN, with the local mass function. Our approach has been to try the simplest solution and then add features to obtain good agreement. In order to include a population of low λ objects and a large spread in possible λ values, we find that at least three populations are required, with different absorption properties depending on intrinsic luminosity for the lowest λ objects. AGN evolution is not a straightforward problem, and may in future require more complex behaviour to be considered. We find that most of the black holes in our solutions have high accretion efficiencies ($\epsilon > 0.1$), and therefore must be spinning rapidly, which has implications for the merger and accretion histories (Volonteri et al. 2005; King & Pringle 2006).

5 ACKNOWLEDGEMENTS

REFERENCES

Babić A., Miller L., Jarvis M. J., Turner T. J., Alexander D. M., Croom S. M., 2007, A&A, 474, 755
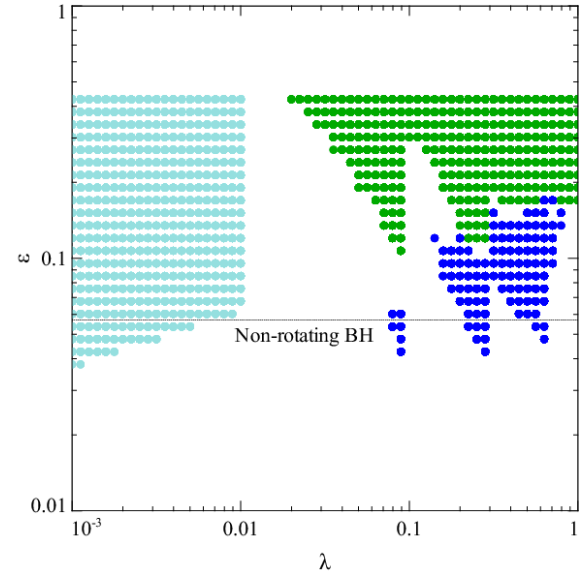Brandt W. N., Hasinger G., 2005, ARA&A, 43, 827

Figure 3. Allowed values of Eddington ratios (λ) and radiative accretion efficiencies (ϵ) for absorbed, blue (light grey and black) and unabsorbed, green (medium grey) AGN. Light blue points (light grey) represent the fraction of absorbed objects that have low Eddington ratios $10^{-3} < \lambda < 10^{-2}$, and dark blue (black) the others $10^{-2} < \lambda < 1$. Unabsorbed objects with $10^{-2} < \lambda < 1$ are plotted in green (medium grey). Each evolved mass function is characterised by a fixed set of three points from the plot.

Cavaliere A., Morrison P., Wood K., 1971, ApJ, 170, 223
Fabian A. C., Iwasawa K., 1999, MNRAS, 303, L34
Fabian A. C., Vasudevan R. V., Gandhi P., 2008, MNRAS, 385, L43
Gilli R., Comastri A., Hasinger G., 2007, A&A, 463, 79
Hasinger G., 2008, A&A, 490, 905
King A. R., Pringle J. E., 2006, MNRAS, 373, L90
Kormendy J., Richstone D., 1995, ARA&A, 33, 581
Lynden-Bell D., 1969, Nat, 223, 690
Magorrian J. et al., 1998, AJ, 115, 2285
Marconi A., Hunt L. K., 2003, ApJ, 589, L21
Marconi A., Risaliti G., Gilli R., Hunt L. K., Maiolino R., Salvati M., 2004, MNRAS, 351, 169
Merloni A., 2004, MNRAS, 353, 1035
Rees M. J., 1984, ARA&A, 22, 471
Richstone D. et al., 1998, Nat, 395, A14
Risaliti G., Maiolino R., Salvati M., 1999, ApJ, 522, 157
Salpeter E. E., 1964, ApJ, 140, 796
Salucci P., Szuszkiewicz E., Monaco P., Danese L., 1999, MNRAS, 307, 637
Schmidt M., 1963, Nat, 197, 1040
Shankar F., Weinberg D. H., Miralda-Escudé J., 2007, ArXiv e-prints, 710
Small T. A., Blandford R. D., 1992, MNRAS, 259, 725
Soltan A., 1982, MNRAS, 200, 115
Tozzi P. et al., 2006, A&A, 451, 457
Treister E., Urry C. M., 2006, ApJ, 652, L79
Treister E. et al., 2008, ArXiv e-prints
Ueda Y., Akiyama M., Ohta K., Miyaji T., 2003, ApJ, 598, 886
Vasudevan R. V., Fabian A. C., 2007, MNRAS, 381, 1235
Volonteri M., Madau P., Quataert E., Rees M. J., 2005, ApJ, 620, 69